Article ID: 1006-8775(2009) 01-0155-07

IMPACTS OF ATOVS DATA ASSIMILATION ON PREDICTION OF A RAINSTORM OVER SOUTHEAST CHINA

WAN Qi-lin (万齐林)[1, 2], Jianjun XU (徐建军)[3], HE Jin-hai (何金海)[1]

(1. Nanjing University of Information Science & Technology, Nanjing 210044 China; 2. Guangzhou Institute of Tropical and Marine Meteorology, CMA, Guangzhou 510080 China; 3. Joint Center for Satellite Data Assimilation (JCSDA) 5200 Auth Road, WWB, Camp Springs, MD 20746, USA)

Abstract: Using the Advanced Research WRF (ARW WRF) model and the Gridpoint Statistical Interpolation (GSI) three-dimensional variational analysis (3DVAR) system, the impact of assimilating ATOVS (Advanced TIROS Operational Vertical Sounder) radiance through the prototype Community Radiative Transfer Model (pCRTM) is evaluated on the forecasting of a heavy rainstorm occurring over the central Guangdong province in the southeast of China on 20-21 June 2005. A pair of comparison experiments (NODA and DA) for this case is conducted with multiple configurations, including nesting domains with 4-km and 12-km grid distances. The results showed that by changing the initial condition through data assimilation, a modified divergence and moisture field with the structure of dipoles has been added to the axis of the rainband with a southwest-northeast orientation. When more moisture carried by a southwesterly low level jet (LLJ) was converged into the northeast portion of the rainband around the observatory station of Longmen, the amplitude of moisture static energy (MSE) increased substantially at low levels much more than at middle levels, resulting in the enlarging of differences in MSE between 500 hPa and 850 hPa; the atmosphere became more unstable. Consequently, the convective rainfall increased in the northeast part of the province around the Longmen station, which was consistent with the observed distribution of rainfall.

Key words: numerical simulation; rainstorm; data assimilation; ATOVS

CLC number: P457.6 **Document code:** A **doi:** 10.3969/j.issn.1006-8775.2009.02.004

1 INTRODUCTION

Strong summertime convective storms over southeast China are frequently associated with maritime tropical air that arrives as part of East Asian Monsoon (EAM, Zhu et. al., [1]). The high spatial variability of monsoon rainfall is related to the particular topography of the region. As Fig. 1 shows, the EAM region is characterized by the Yunnan-Guizhou Plateau (e.g. southeast branch of the Tibetan Plateau) in the west, the Pacific Ocean in the east and the South China Sea in the south. With the arrival of the EAM, extreme storms can occur through deep convection over there and result in hydrological disasters, such as flash flooding. Improving the forecast of extreme storms in this area, therefore, is receiving great attention in the hydrometeorological community. In practice, however, the numerical forecast of such deep convective systems are largely validated poorly (Ding [2]). As we know, weather forecast may fail after a certain period of forecast duration. One reason for the failure is attributed to the errors of initial conditions (Lorenz [3]). It means that an arbitrarily small error in the analysis of the initial state of the atmosphere can have an overwhelming effect in a finite amount of time. Therefore, it is not surprising that considerable effort has been made on improving the estimates of the initial model states through sophisticated techniques. One of such techniques is the three-dimensional variational (3DVAR) data assimilation method using satellite radiance.

The assimilation of satellite radiance observations into a numerical weather prediction (NWP) system is an important path to improve weather forecasts by providing initial conditions representative of the true

Received date: 2009-02-20; **revised date:** 2009-06-25
Foundation item: National Natural Science Foundation of China (NSFC) General Program (40775058); National Special Research Project for Non-profit Industry (GYHY200706014)
Biography: WAN Qi-lin, professor, mainly conducting research on numerical weather prediction and tropical weather & climate.
E-mail for correspondence author: qlwan@grmc.gov.cn

state of the atmosphere. There are two basic approaches to assimilate satellite information into a data assimilation system (DAS); the first approach is to assimilate the retrieved data from radiances measured by satellite instruments and the second is to assimilate the radiance measurements directly into a DAS. The direct radiance assimilation is theoretically superior to the retrieval assimilation because the observational error statistics are more justified in the direct radiance assimilation than in the retrieval assimilation (Eyre et al. [4]; Derber and Wu [5]; McNally et al., [6]). The purpose of this paper is to investigate how the direct assimilation of radiance into a full physics mesoscale model affects the forecasts of a rainstorm. In this paper, both the Gridpoint Statistical Interpolation (GSI) analysis system and the prototype Community Radiative Transfer Model (pCRTM) within a complete data assimilation system are linked to the ARW WRF mesoscale system. The rainstorm event is presented in section 2. Section 3 and section 4 describe the data assimilation system, experiments design, and the ATOVS datasets. The impact of the ATOVS data assimilation on the rainfall forecasts are evaluated in section 5. The discussion and summary are provided in sections 6 and 7, respectively.

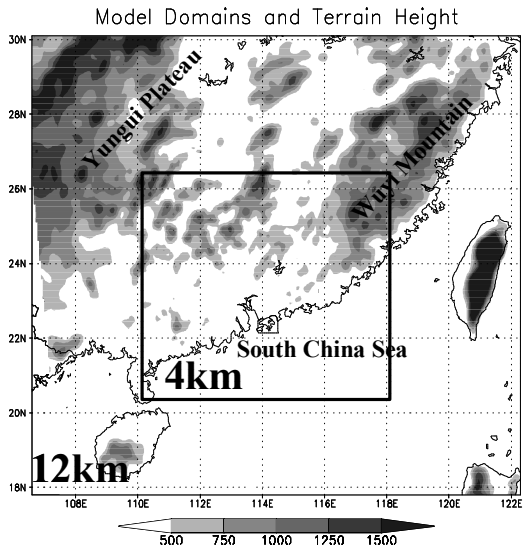

Fig.1 Domains for the ARW WRF forecasts. The outside box is the coarse grid (domain 1) with 12-km spacing; the inner box is the nested grid (domain2) with 4-km spacing. The shading shows the elevation of terrain (Unit: meter).

2 EVENT

From the observed rain gauge data, we found that a strong rainstorm occurred in the central Guangdong province between the Jiulian and Lianhua Mountains over the southeast of China during 18–25 June 2005, and the amount of weekly rainfall exceeded 1300 mm in some of the observatory stations. The 24-hour rainfall averaged from 0600 UTC 20 through 0600 UTC 21 June 2005 indicates (Fig. 3a) the presence of a rainband with the southwest-northeast axis going through the observatory stations of Conghua and Longmen and the appearance of a center of strongest rainfall in the areas around the Longmen station. The time series of hourly precipitation (Fig. 3b) averaged over the storm center (heaven box in Fig. 3a) shows the presence of several peaks of hourly precipitation over 20 mm/h from 2100 UTC 20 June 2006.

3 MODEL AND EXPERIMENT DESIGN

The weather model used in this study is the Advanced Research WRF (ARW WRF) model (Michalakes et al. [7]; Skamarock et al. [8]), which is a nonhydrostatic, fully compressible, primitive equation model. The Gridpoint Statistical Interpolation (GSI) analysis system is being developed based on NCEP's current three-dimensional variational analysis (3DVAR) system named as Spectral Statistical Interpolation (SSI) (Parrish and Derber [9]).

The current GSI regional analysis system accepts the NCEP's Nonhydrostatic Mesocale Model (NMM) WRF and the ARW WRF mass core of NCAR, and the input data could be either in the binary or NetCDF format. Interface is specialized separately for the WRF NMM core and the WRF mass core. For the ARW WRF mass core, the mass variables (T, Q) do not need to be interpolated, but wind variables do, with the zonal component (u) interpolated in x to mass points and meridional component (v) interpolated in y to mass points. However, this is minimized by interpolating only the analysis increment back to the original grid and adding to the input guess.

The US Joint Center for Satellite Data Assimilation (JCSDA) has developed its beta version of the community radiative transfer model (CRTM). The GSI 3DVAR data assimilation used in the current study is referred to as the prototype CRTM (pCRTM), which is generated from a fast radiative transfer model known as Optical Path Transmittance (OPTRAN). The OPTRAN model (McMillin, et al. [10]) computes atmospheric transmittance by predicting, by means of regression, the absorption coefficient for each absorbing species on the absorber path for that species.

In the ARW WRF regional model, the physics of the model includes the Eta Ferrier microphysics scheme, Yosei University's planetary boundary layer (PBL) scheme, 5-layer thermal diffusion land surface scheme, Rapid Radiative Transfer Model longwave radiation, and Dudhia shortwave radiation scheme. A nesting domain with 4-km and 12-km resolution has been used in these experiments (Fig. 1). The vertical 31-level σ

values are 1.000, 0.993, 0.980, 0.966, 0.950, 0.933, 0.913, 0.892, 0.869, 0.844, 0.816, 0.786, 0.753, 0.718, 0.680, 0.639, 0.596, 0.550, 0.501, 0.451, 0.398, 0.345, 0.290, 0.236, 0.188, 0.145, 0.108, 0.075, 0.046, 0.021, 0.000.

A deep convective rainstorm event occurring in the southeast of China during 0600 UTC 20 through 0600 UTC 21 June 2005 was chosen for the case study. A pair of parallel experiments has been conducted. The control experiment (referred to as NODA) was conducted with the initial condition from the GFS forecasts at 0600 UTC 20 June 2005 and run for 24 hours. The lateral boundary conditions from the operational GFS forecast are at 3-h intervals. The data assimilations experiment (referred to as DA) was performed in two steps: firstly, the GSI data assimilation system is used with the ATOVS datasets including AMSU-A/B and (HIRS)/3 to modify the initial condition at 0600 UTC 20 June 2005, and then, the ARW WRF forecast model is run in the same way as the control experiment.

4 ATOVS DATA

The ATOVS (i.e., Advanced Television and Infrared Observation Satellite (TIROS)-N Operational Vertical Sounder) radiance data was supplied by NESDIS. The ATOVS is composed of Advanced Microwave Sounding Unit (AMSU) and High-Resolution Infrared Sounder (HIRS)/3. Two separate radiometers (AMSU-A and AMSU-B) compose the AMSU platform. The AMSU-A is a cross-track, stepped-line scanning total power radiometer. The instrument has an instantaneous field-of-view of 3.3° at the half-power points, providing a nominal spatial resolution at nadir of 48 km. The AMSU-B is a cross-track, continuous line-scanning, total-power radiometer with an instantaneous field-of-view of 1.1° (at the half-power points). Spatial resolution at nadir is nominally 16 km. The antenna provides cross-track scans, scanning ±48.95° from nadir with a total of 90 earth fields-of-view per scan line.

The primary function of the 15-channel AMSU-A (channels 1 – 15) is to provide temperature sounding of the atmosphere; three of the channels will also provide information on tropospheric water vapor, precipitation over the ocean, sea-ice coverage, and other surface characteristics. The five channels of the AMSU-B (channels 16 – 20) mainly measure water vapor and liquid precipitation over land and sea. The HIRS/3 is a 20-channel instrument that has an instantaneous field-of-view of 1.3° providing a nominal spatial resolution at nadir of 18.9 km. The antenna provides cross-track stepped scans, scanning ±49.5° from nadir with a total of 56 fields-of-view per scan line. The instrument completes one scan line every 6.4 s.

4.1 *Bias correction*

Before becoming available for usage, these data have gone through substantial preprocessing by NESDIS, referred to as bias correction, with the surface emissivity statistically limb corrected and (adjusted to nadir) corrected in the microwave channels of AMSU-A and AMSU-B and cloud cleared in the tropospheric (HIRS)/3 channels. As the source of the biases could be instrument-calibrated, correction had been made in the predictor and zenith angle. Dependent on the satellite sensor, the biases are not constant for each channel. For example, it is shown that the innovation (defined as the observation minus the model) of brightness temperature is a function of the channels and has been reduced for the whole studied regional set of observations after the bias correction (figure omitted). With the bias correction, the innovation for most channels is quite small, less than 2° in terms of brightness temperature, and its magnitude is much smaller than the value without bias correction. So the best way to account for the bias is to remove all problems of satellite calibration and ground processing.

4.2 *Quality Control*

Derber and Wu[5] pointed out that the presence of a single data point containing large errors can result in substantial degradation of the analysis and subsequent forecast. For this reason, a simple quality control has been developed and the observed brightness temperature data has been modified empirically with various parameters for the different instruments. In the GSI analysis system, the check will include two steps: Firstly, the location check includes the removal of observations outside the domain and thinning procedure, the exclusion of location/time duplicates and incomplete observations, and the ensuring of vertical consistency of upper-air profiles. Secondly, numerous quality control (QC) checks are redone based on the various quality parameters after the modeled brightness temperature is obtained through the radiative transfer model. These quality parameters are used in terms of the expected observational error variance as a function of channels and are adjusted by the position across the track of the scan, whether it is over land, sea, snow, sea ice or a transitional region, the elevation, the difference between the model and the real topography, and the latitude. For example, in the AMSU-A of NOAA 16 (Fig. 2), the quality parameter has been modified due to the error of transmittance at the top of the model, high topography (greater than 2000 m) and the differences between the window channel observations and the simulated ones. The used radiance shows that without

the QC, the maximum radiance in NOAA 16 becomes 2715 pixels (Fig. 2a); In contrast, under the QC, it is only 350 pixels (Fig. 2b).

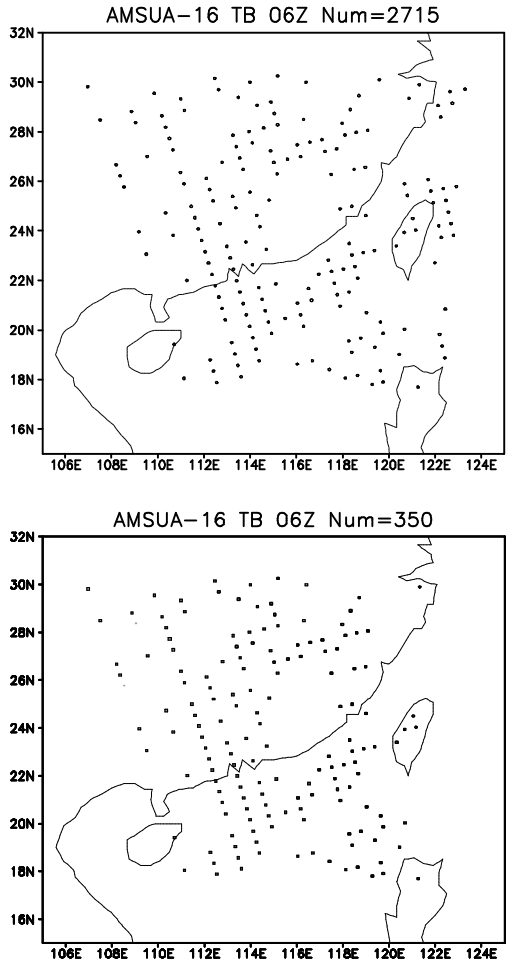

Fig.2 Model domain and ATOVS (AMSU-A/B, and (HIRS)/3) radiance has been used in the current data assimilation system at 0000 UTC 27 August 2005 and the inner box shows the nesting model domain. Upper panel: before quality control (QC); lower panel: after QC.

It is obvious that the bias correction and quality control can reduce the innovation of brightness temperature, beneficial to the minimization procedure in the data assimilation system. However, due to the imperfectness of the bias correction and quality control schemes, a lot of true observation data has been tossed out, making it worthwhile to study desirable schemes for bias correction and quality control in the future work.

5 RAINFALL FORECASTS

For the 24-h forecasts starting from 0600 UTC 20 June 2005, the rainfall produced from the control experiment (NODA) (Fig. 3c) and from the ATOVS radiance experiment (DA) (Fig. 3d) is compared with the rain gauge observations (Fig. 3a). The results indicate that without data assimilation (NODA), the prediction cannot identify the correct location of the heavy storm centered over the Longmen station (Fig. 3c), the forecasted rainfall center is deviated to the southwest around the Conghua station from the observed location, and the rainfall intensity is also a little higher than the observation. In contrast, the DA improves somewhat the rainfall distribution (Fig. 3d) and corrects the maximum rainfall center to more to the right over the Longmen station. The extension axis of the rainband from southwest to northeast is reproduced although it does not match the observation completely.

It is clearly shown that the DA improves the simulated rainfall location in the northeast - southwest rainband and produces a closest rainfall amount over the northeast area; however, there is still an eastward shift in terms of the position of the rainband. The DA simulates relatively proper locations of the rainband but misses slightly the maximum rainfall center. This suggests that the satellite data assimilation plays an important role in the simulation of the rainband. The ATOVS radiance can correct the rainfall location in DA experiments although it shifts the location of the maximum rain northeastward.

To examine the effect of the DA analysis on the rainfall prediction, a statistical variable, equitable threat score (ETS), is calculated against the observed rainfall data over the central area of the rainstorm. The results for the precipitation thresholds of 4 mm are presented in Fig. 4. With the radiance data assimilation, the ETS is slightly higher than its counterpart in NODA for the whole forecasting period. The improvement on the rainfall prediction through the DA extends beyond the 6-h forecast. The highest threat score is obtained in the 15-h forecast in DA experiments.

From this statistical result (Fig. 4), it is suggested that the assimilation of radiance produces better short-range precipitation forecast. The improvement is mainly limited to the forecast range of about 20 hours in this case study.

6 DISCUSSION

Before discussing the impact of ATOVS radiance data assimilation on the forecasts, we first look at the preliminary feature of initial fields in the control experiment (NODA). In order to clearly understand the initial condition for the rainstorm, we focus on the wind flow in the low level of 850 hPa. At the initial time (0600 UTC 20 June 2005), there was a strong southwesterly low level jet (LLJ) with wind speeds over 12 m/s prevailing in the area between Jiulian and Lianhua Mountains. The line of strongest wind speed paralleling to the Jiulian Mountain is just located to the northwest side of the rainband (Fig. 5a vs. Fig. 3). It is

clear that the LLJ is closely related to the activity of the rainstorm through providing the essential moisture.

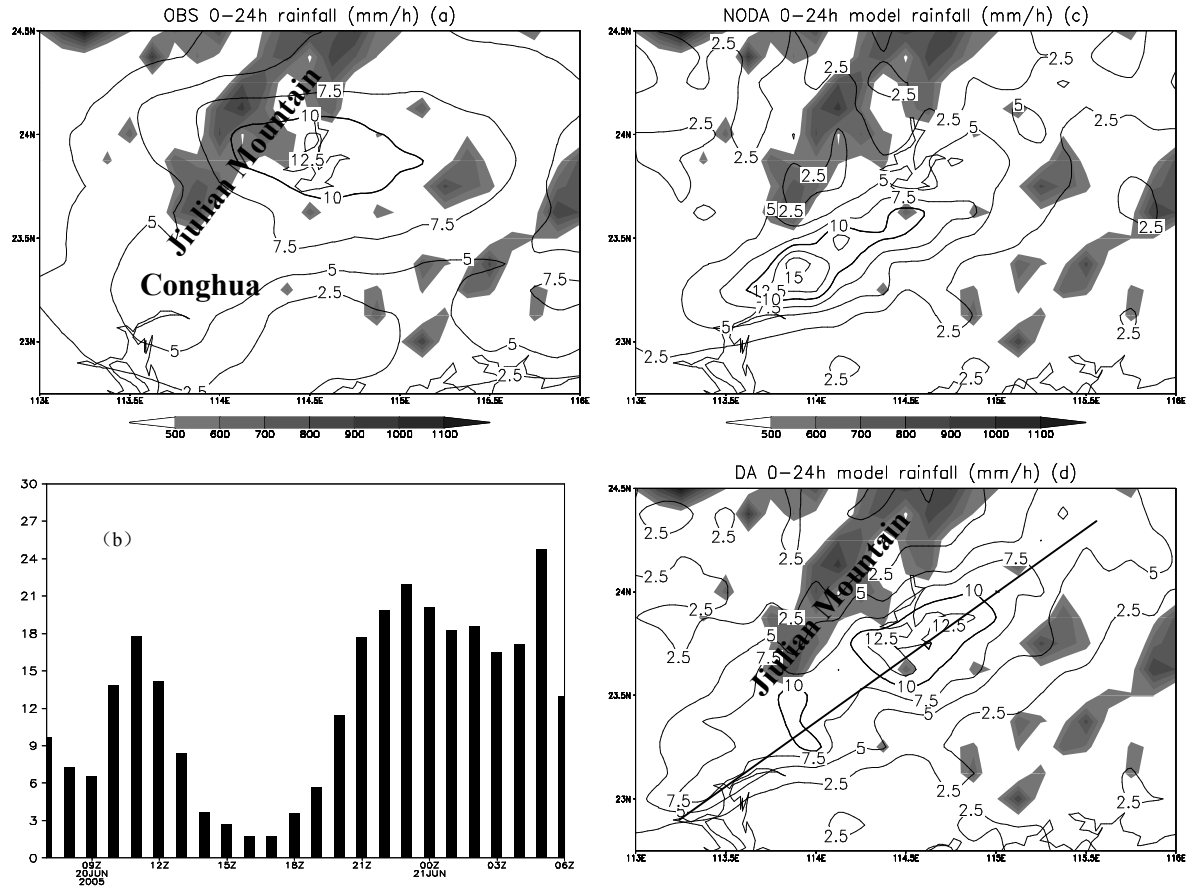

Fig.3 0-24 hour precipitation of observation and model (Unit: mm/hour), (a) 24-hour averaged observational rainfall from 0600 UTC 20 through 0600 UTC 21 June 2005; (b) Time series of hourly averaged rainfall over the rainstorm central areas in the panel above; (c) same as (a) but for model forecasts without data assimilation (NODA); (d) same as (a) but for model forecasts with data assimilation (DA). Shading indicates the elevation of local terrain. (Unit: meter)

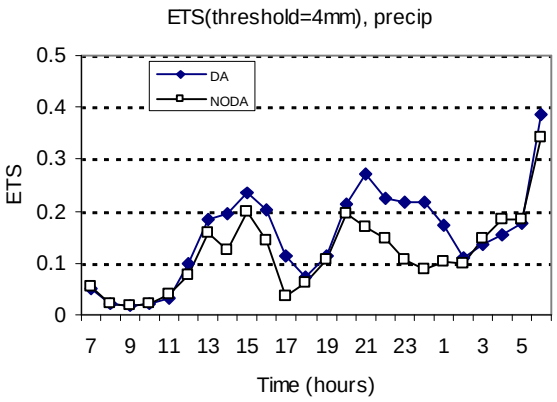

Fig.4 Time series of equitable threat score (ETS) for precipitation.

We now consider a question: what happens with the ATOVS radiance initialization? First of all, for the precipitation, with the (DA) compared to the NODA, evidence is observed that the distribution of rainfall changed greatly (shown as shades in Fig. 5a). The maximum difference (defined as DA minus NODA and the same hereafter) in rainfall appeared in a different location relative to the rainband, i.e., positive in the southeast side of the rainband around the observatory station of Conghua and negative in the northwest side of the rainband around the Jiulian Mountain. Please note the presence of a feature: the maximum increase is located just over the central area of the rainstorm.

Corresponding to the changes in precipitation, the prediction of the divergence field is modulated by the radiance assimilation. The 24-h forecast of divergence differences at 850 hPa shows (Fig. 5b) a positive dipole structure in the southwest (around the observatory station of Conghua) and a negative one in the northeast (around the area of Longmen station), following the axis of the rainband. It is not difficult to

find that the difference divergence outflow at low levels reduces the convection in Conghua and the difference convergence inflow beneath enhances the rainstorm in Longmen, which is well consistent with the distribution of rainfall (Fig. 3).

For the moisture, 24-h forecasts of the total moisture content integrated from the surface through 500 hPa (Fig. 5c) are consistent with the anomalous divergence field. The difference field (shaded) indicates that the moisture content increases over the area of the active center of the rainstorm and decreases over the southwestern area.

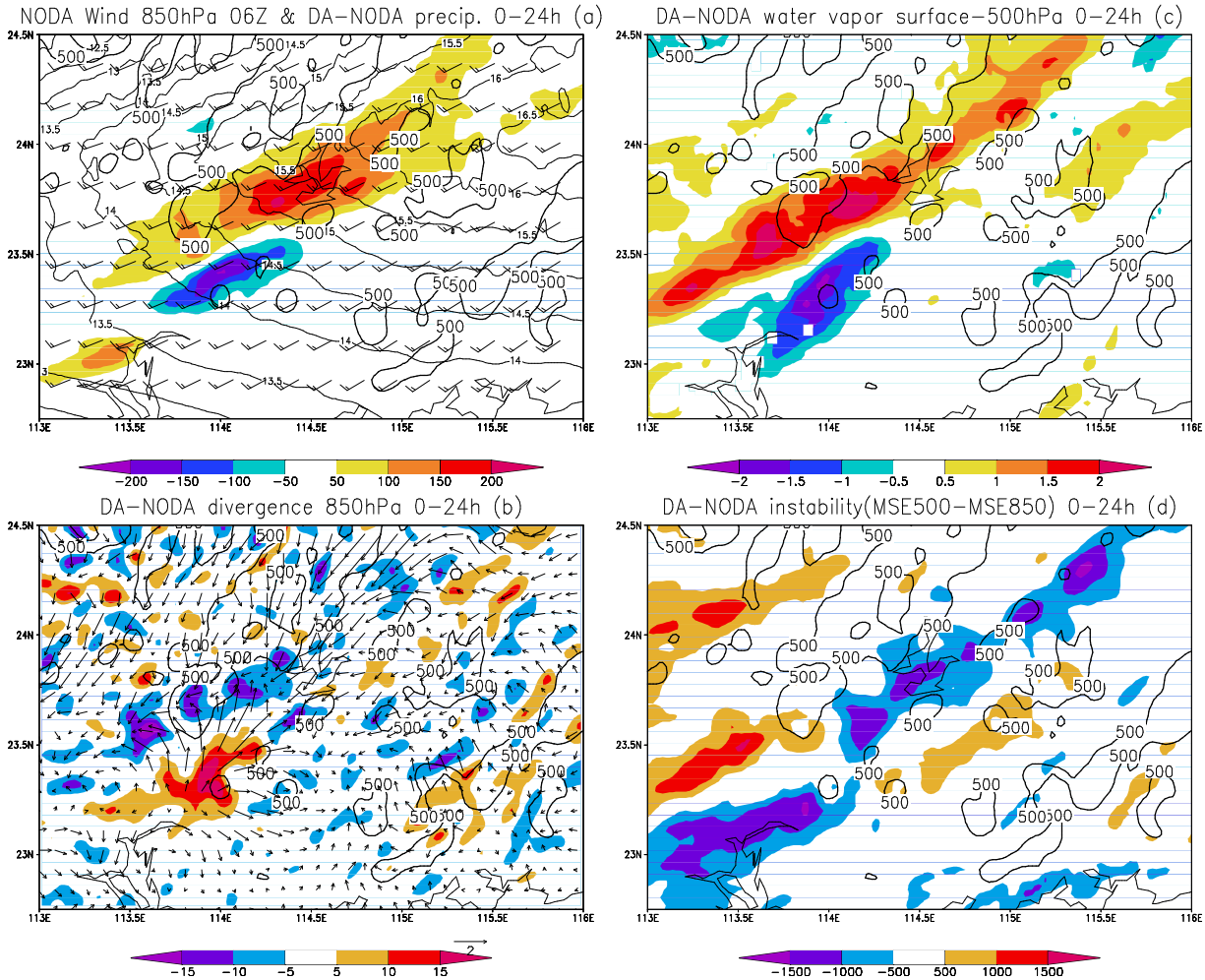

Fig.5 (a) Wind speed (thin contour, unit: m s^{-1}) on 850 hPa at initial time (0600 UTC 20) and difference of precipitation (shaded) for 24-hour averaged from 0600 UTC 20 through 0600 UTC 21 June 2005, the heavy dished line indicates the ridge of high wind speed; (b) difference of divergence (shaded) on 850 hPa (unit:$10^{-5}s^{-1}$) for the 24-hour average, and the vector indicates the corresponding difference wind field (unit: m s^{-1}); (c) difference of water vapor (shaded) integrated from surface through 500 hPa for the 24-hour average (unit: g/kg) ; (d) difference of instability (shaded) for the 24-hour average, and the instability is defined by the difference of moisture static energy (MSE) between 500 hPa and 850 hPa (unit: J kg^{-1}). Note, the heavy contours indicate the elevation of local terrain (Unit: meter). The difference is expressed by DA minus NODA. '+' is positive and ' - ' is negative.

With the changing of moisture content around the rainband, moisture static energy (MSE) increases in the northeast (around the Longmen station) at the low level (850 hPa) but decreases at the middle level (500 hpa); the instability expressed by the MSE difference between 500 hPa and 850 hPa shows that the convective system operating between these two levels becomes more unstable (Fig. 5d). In this way, the anomalous moisture conditions tend to increase the frequency (via an increase in instability) and magnitude (via an increase in the MSE) of convective rainfall around the Longmen station. Meanwhile, it should be noted that in spite of similar instability increases in the southwest around the Conghua station, however, the low level anomalous divergence flow (Fig. 5b) reduces the moisture content (Fig. 5c) and leads to the decrease of rainfall over there.

Based on the above analysis, it is found that after

the initialization of radiance, the intensity and structure of the initial field, including the atmospheric flow, moisture, and instability, have been modified significantly. An anomaly of the dipole structure in the southwest-northeast direction has been added over the rainband, which corrects the location of rainfall.

7 SUMMARY

On 20–21 June 2005, a series of mesoscale convective systems developed along the central Guangdong Province between Jiulian and Lianhua Mountains over the southeast of China. Based on the heavy rainstorm case, using the JCSDA GSI regional data assimilation system, we investigated the impact of the ATOVS radiance assimilation on the 24-h forecast of precipitation, with the results showing that the DA produces relatively proper locations of the rainband but misses the center of maximum rainfall slightly. The ETS result suggests that the assimilation of radiance produces better short-range precipitation forecast. The improvement is mainly limited to the forecast range of about 20 hours in this case study.

With the change in the initial condition, radiance assimilation generates more realistic wind divergence, moisture field, and instability, and an anomaly with dipole structure is added to the location of the rainstorm. The amplitude of MSE increases much more at low levels than at mid levels in the northeast portion of the rainband; as a result of the increased difference in MSE between 500 hPa and 850 hPa, the atmosphere becomes more unstable. Consequently, anomalous moisture condition tends to modulate the distribution of convective rainfall, increasing it in the northeast (around the Longmen station) and decreasing it in the southwest (around the Conghua station).

Results from this case study showed that radiance assimilation using the GSI regional system could improve the model rainfall forecast, but the impact was not as much as we expected. Due to the complexity of the parameterization of rainfall processes and lack of knowledge in the quality control of satellite observation errors, more attention should be paid to the limitations of data assimilation.

Parameterization of rainfall processes plays a significant role in simulating various large-scale and mesoscale phenomena. The minimization procedure of data assimilation is sensitive to horizontal distance resolution and microphysics options. For this convective case, the 4-km model distance and Eta Ferrier microphysics scheme seem to work well for the rainstorm forecasts over the southeast of China.

Finally, this conclusion is just from one kind of satellite radiance data. There are still lots of other radiances that can be used to improve rainfall forecasts.

***Acknowledgement*:** The authors would like to thank U.S. Joint Center for the Satellite Data Assimilation for providing the GSI data assimilation system.

REFERENCES:

[1] ZHU Qian-gen, LIN Jing-rui, SHOU Shao-wen, et al. Principles and Methods in Synoptic Meteorology [M]. Beijing: China Meteorological Press, 1981: 535 pp.

[2] DING Y H. Summer monsoon rainfalls in China [J]. J. Meteor. Soc. Japan, 1992, 70: 337-396.

[3] LORENZ E N. The mechanics of vacillation [J]. J. Atmos. Sci., 1963: 20: 448-465.

[4] EYRE J R, KELLY G, MCNALLY A P, et al. Assimilation of TOVS radiances through one dimensional variational analysis [J]. Quart. J. Roy. Meteor. Soc., 1993: 119: 1427-1463.

[5] DERBER J C, WU Wan-shu. The Use of TOVS Cloud-Cleared Radiances in the NCEP SSI Analysis System [J]. Mon. Wea. Rev., 1998, 126, 2287-2299.

[6] MCNALLY A P, DERBER J C, WU W, et al. The use of TOVS level-1b radiances in the NCEP SSI analysis system [J]. Quart. J. Roy. Meteor. Soc., 2000, 126: 689-724.

[7] MICHALAKES J, CHEN S, DUDHIA J, et al. Development of a next generation regional weather research and forecast model [M]// ZWIEFLHOFER W, KREITZ N. Developments in Teracomputing: Proceedings of the Ninth ECMWF Workshop on the Use of High Performance Computing in Meteorology, World Scientific, 2001: 269-276.

[8] SKAMAROCK W C, KLEMP J B, DUDHIA J, et al. A description of the Advanced Research WRF Version 2 [R]. NCAR Tech. Note NCAR/TN-468+STR, 2005, 94 pp.

[9] PARRISH D F, DERBER J C. The National Meteorological Center's spectral statistical interpolation analysis system [J]. Mon. Wea. Rev., 1992, 120: 1747-1763.

[10] MCMILLIN L M, CORE L J, KLEESPIES T J. Atmospheric transmittance of an absorbing gas. 5: Improvements to the OPTRAN approach [J]. Appl. Opt., 1995, 34: 8396-8399.

Citation: WAN Qi-lin, Jianjun XU and HE Jin-hai. Impacts of ATOVS data assimilation on prediction of a rainstorm over southeast China. *J. Trop. Meteor.*, 2009, 15(2): 155-161.